JCM
Journals.ASM.org

Subcutaneous Phaeohyphomycotic Nodule Due to *Phialemoniopsis hongkongensis* sp. nov.

Chi-Ching Tsang,[a] Jasper F. W. Chan,[a,b,c,d] Philip P. C. Ip,[e] Antonio H. Y. Ngan,[a] Jonathan H. K. Chen,[a] Susanna K. P. Lau,[a,b,c,d] Patrick C. Y. Woo[a,b,c,d]

Department of Microbiology,[a] State Key Laboratory of Emerging Infectious Diseases,[b] Research Centre of Infection and Immunology,[c] Carol Yu Centre for Infection,[d] and Department of Pathology,[e] The University of Hong Kong, Hong Kong

Phialemoniopsis **species are ubiquitous dematiaceous molds associated with a wide variety of superficial and systemic infections in human. In this study, we isolated a mold from the forearm nodule biopsy specimen from a patient with underlying liver cirrhosis, ankylosing spondylosis, and tuberculosis. He was treated with itraconazole, but unfortunately, he succumbed as a result of disseminated tuberculosis with multiorgan failure. The histology results of the skin biopsy showed necrotizing granulomas in which numerous fungal elements were found. On Sabouraud dextrose agar, the fungal isolate grew as white-to-cream and smooth-to-velvety colonies. Microscopically, oval-to-cylindrical conidia were observed from abundant adelophialides, which possessed barely visible parallel collarettes but no basal septa. The azole drugs voriconazole, itraconazole, and posaconazole, as well as amphotericin B, showed high activities against this fungus. Internal transcribed spacer, 28S nuclear ribosomal DNA (nrDNA), and β-actin and β-tubulin gene sequencing showed that this fungus is most closely related to but distinct from** ***Phialemonium curvata*****. Matrix-assisted laser desorption ionization–time of flight mass spectrometry (MALDI-TOF MS) and hierarchical cluster analysis showed that the MALDI-TOF MS spectrum of this fungus is most closely related to that of** ***Phialemonium pluriloculosa*****. We propose a new species,** ***Phialemoniopsis hongkongensis*** **sp. nov., to describe this fungus.**

Phialemoniopsis is a newly established anamorphic genus that accommodates filamentous fungi with morphological features resembling *Phialemonium* species. It currently contains four species, namely, *Phialemoniopsis cornearis*, *Phialemoniopsis curvata*, *Phialemoniopsis ocularis* (type species), and *Phialemoniopsis pluriloculosa* (1). Members of this genus are widely distributed in the environment, having been isolated from air, industrial water (2), plant materials (3–5), river water, sewage, and soil (2), making these fungi emerging opportunists for causing human infections. *Phialemoniopsis* species have been detected in different continents, including Africa (4), the Americas (1–3, 6–16), Antarctica (2), Asia (5, 17–21), and Europe (2, 22–25). Although *Phialemoniopsis* species grow as pale colonies, melanin has been detected in their hyphae, and therefore, infections due to these dematiaceous molds are considered to be phaeohyphomycosis (6). *Phialemoniopsis* species have been reported to cause endocarditis and endovascular infections (9, 17, 20, 22), endophthalmitis and keratitis (2, 15, 16, 18, 19), fungemia (7, 12, 24), meningitis (21), septic arthritis and spondylodiscitis (10, 23), and skin and soft tissue infections (1, 6, 8, 25) in humans, with some cases being fatal infections. In addition, they have been isolated from various clinical specimens, including those from cerebrospinal fluid, corneal and vitreous fluid, peritoneal dialysis catheter, sinus, skin lesions and nails, and synovial fluid, although the clinical details of the patients were not presented (1, 2, 13). *Phialemoniopsis* species are also opportunistic animal pathogens, having caused pleural effusion in a dog (11), and they were isolated from the coarse outer fur of sloths (14).

Recently, we isolated a mold from a necrotizing granulomatous forearm nodule biopsy specimen. Microscopic examination of the fungal culture was not conclusive. Internal transcribed spacer (ITS) sequencing showed that it was clustered with, but significantly different from, known *Phialemoniopsis* species. Therefore, we hypothesized that the isolate may represent a novel fungal species. To test the hypothesis, we performed additional phenotypic and genotypic characterization on the isolate and compared its characteristics with those of closely related fungal species. On the basis of the findings, we propose a new species, *Phialemoniopsis hongkongensis* sp. nov., to describe this fungus. Identification of *Phialemoniopsis* species by gene sequencing, phenotypic characterization, and matrix-assisted laser desorption ionization–time of flight mass spectrometry (MALDI-TOF MS) were discussed.

MATERIALS AND METHODS

Patient and strains. This study has been approved by the Institutional Review Board of the University of Hong Kong/Hospital Authority Hong Kong West Cluster. All clinical data of the index patient were collected by retrieving and analyzing the patient's hospital record. Clinical specimens were collected and handled according to standard protocols and were grown on Sabouraud dextrose agar (SDA) (Oxoid, United Kingdom) with chloramphenicol (50 μg/ml) (Sigma-Aldrich, St. Louis, MO, USA) at 37°C to obtain the case isolate HKU39^T. The reference strains *P. cornearis* CBS 131711^T, *P. curvata* CBS 490.82^T, *P. ocularis* CBS 110031^T, and *P. pluriloculosa* CBS 131712^T were obtained from the Centraalbureau voor Schimmelcultures of the Royal Netherlands Academy of Arts and Sciences (CBS-KNAW Fungal Biodiversity Centre), the Netherlands.

Received 4 June 2014 Returned for modification 13 June 2014
Accepted 23 June 2014
Published ahead of print 25 June 2014
Editor: D. W. Warnock
Address correspondence to Susanna K. P. Lau, skplau@hku.hk, or Patrick C. Y. Woo, pcywoo@hku.hk.

doi:10.1128/JCM.01592-14

Phenotypic characterization. The fungal strain HKU39^T was inoculated onto potato dextrose agar (PDA) (Difco, BD Diagnostic Systems, Sparks, MD, USA) with chloramphenicol (50 μg/ml) for fungal culture as the inoculum for other procedures. Slides for microscopic examination were prepared by the agar block smear preparation method we described previously (26). HKU39^T was also examined by scanning electron microscopy, performed according to our previous publication (27), with modifications. An enzyme activity test was performed using the API-ZYM system (bioMérieux, France), and a carbohydrate assimilation test was performed using the API 20 C AUX system (bioMérieux, France), according to the manufacturer's protocols. For HKU39^T and the reference strains, the effect of different temperatures on growth on PDA was studied, as described in our previous publication (28).

DNA extraction, ITS, partial 28S nrDNA, partial β-actin, and β-tubulin gene sequencing, comparative sequence identity analyses, and phylogenetic analyses. Fungal DNA extraction, PCR amplification, and DNA sequencing of the ITS, partial 28S nrDNA, and partial β-actin and β-tubulin genes for the patient isolate HKU39^T and the reference strains were performed according to our previous publications (28), using the primer pairs ITS1/ITS4 (29) for the ITS, NL1/NL4 (30) for the 28S nrDNA, LPW26272/LPW26273 (designed in this study by selecting the conserved regions from the alignment of the β-actin gene sequences of *Phialemoniopsis* species) for the β-actin gene, and TUB2-F/TUB2-R (31) for the β-tubulin gene. The sequences of the PCR products were comparatively analyzed by pairwise alignment, with the optimal Global alignment parameters, using BioEdit 7.2.0 (32). The sequences of the PCR products were also compared with sequences of closely related species from GenBank by multiple sequence alignment using MUSCLE 3.8 (33) and then were end trimmed. Poorly aligned or divergent regions of the aligned end-trimmed DNA sequences were removed using Gblocks 0.91b (34, 35), with relaxed parameters. Tests for substitution models and phylogenetic tree construction, by the maximum likelihood method, were performed using MEGA 6.06 (36).

MALDI-TOF MS. MALDI-TOF MS was performed according to our previous publication (37), with modifications. Briefly, fungal cells were cultured in 10 ml of Sabouraud dextrose broth (Oxoid, United Kingdom). The cells were then harvested and washed with 1 ml of distilled water. The pellet was resuspended in 300 μl of distilled water and 700 μl of absolute ethanol. The mixture was vortexed and centrifuged at 14,000 rpm for 5 min. The supernatant was removed, and the pellet was air-dried for 2 h. The pellet was then resuspended in 50 μl of 70% formic acid (Sigma-Aldrich) and an equal volume of acetonitrile (Fluka, Switzerland), followed by centrifugation at 14,000 rpm for 5 min. One microliter of the supernatant was transferred to an individual spot on the MSP 96-well polished steel BC target plate (Bruker Daltonics, Germany). Each spot was further overlaid with α-cyano-4-hydroxycinnamic acid (HCCA) matrix (Sigma-Aldrich). The target plate was then analyzed by the microflex LT system (Bruker Daltonics). A protein profile from each spot, with *m*/*z* values of 3,000 to 15,000, was generated. The profiles were analyzed using the MALDI Biotyper 3.1 software (Bruker Daltonics). A representative spectrum of each strain was further selected for hierarchical cluster analysis using ClinProTools 3.0 (Bruker Daltonics).

Antifungal susceptibility test. The susceptibility of HKU39^T to six different antifungal drugs was tested using the Sensititre YeastOne plates (Trek Diagnostic Systems, United Kingdom), according to the manufacturer's protocol for *Aspergillus* species and our previous publication (38).

Nucleotide sequence accession numbers. The ITS, partial 28S nrDNA, and partial β-actin and β-tubulin gene sequences of HKU39^T and the reference strains have been deposited in GenBank with the accession numbers KJ573442 to KJ573461.

RESULTS

Index patient. A 55-year-old Chinese construction site worker had noticed a nodule on his right forearm for 6 months. This right forearm nodule had appeared and progressively enlarged over the

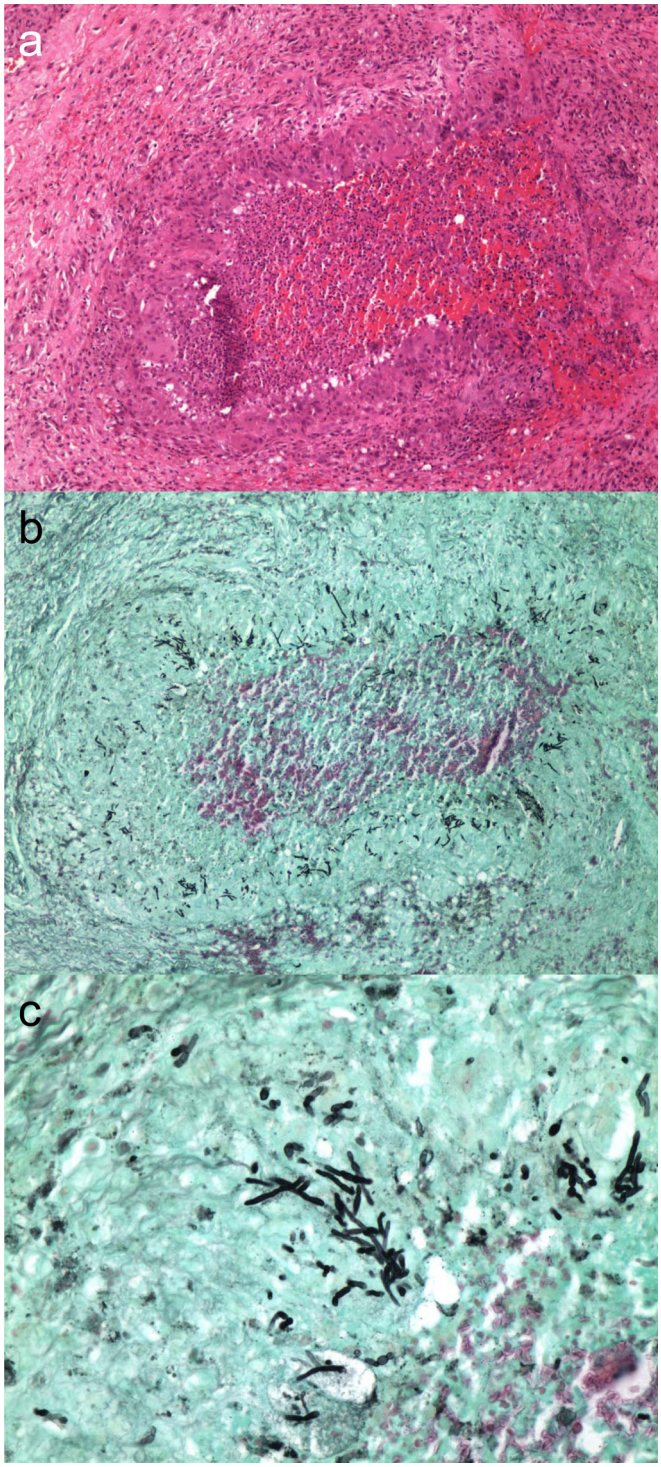

FIG 1 (a) Photomicrograph of the biopsied right forearm nodule showing a necrotizing granuloma with necrotic debris and acute inflammatory cells surrounded by epithelioid histiocytes and occasional multinucleated giant cells (hematoxylin and eosin stain, original magnification, ×10). (b) Photomicrograph of the same field showing numerous fungal elements near the necrotizing granuloma (Grocott's methenamine silver stain, original magnification, ×10). (c) Magnified section of panel b (Grocott's methenamine silver stain, original magnification, ×40).

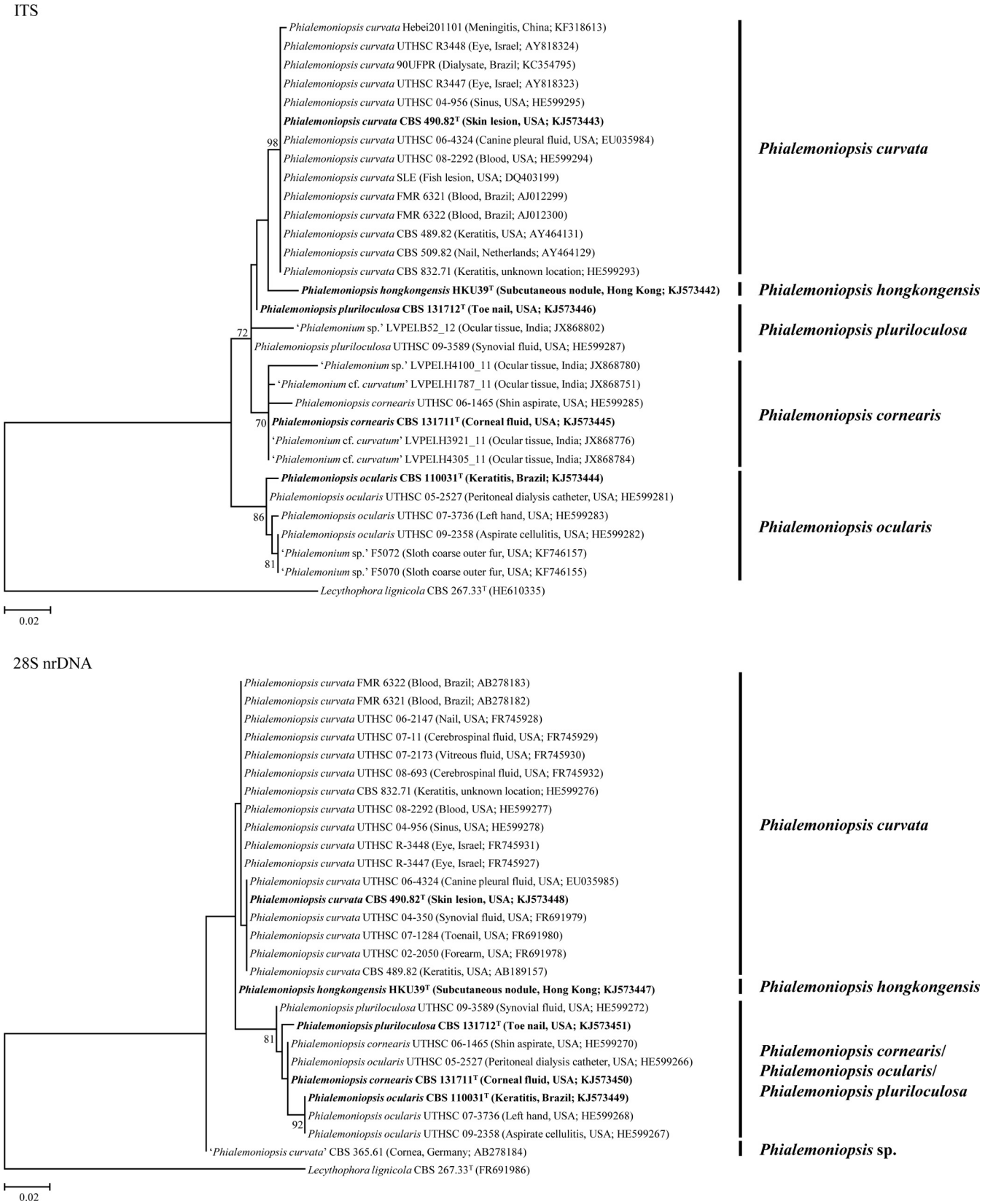

FIG 2 Phylogenetic trees showing the relationship of *P. hongkongensis* to its closely related species. The trees were inferred from ITS and partial 28S nrDNA, β-actin gene, and β-tubulin gene sequence data by the maximum likelihood method with the substitution model K2 (Kimura 2-parameter model) + G (gamma-distributed rate variation) (ITS and partial 28S nrDNA) or TN93 (Tajima-Nei model) + G (partial β-actin and β-tubulin genes). The scale bars indicate the estimated numbers of substitutions per base. The numbers at the nodes indicate the levels of bootstrap support calculated from 1,000 trees, and bootstrap values of <70 are not shown. All names and accession numbers are given as cited in the GenBank database. The sequences that were newly obtained in this study are highlighted in bold.

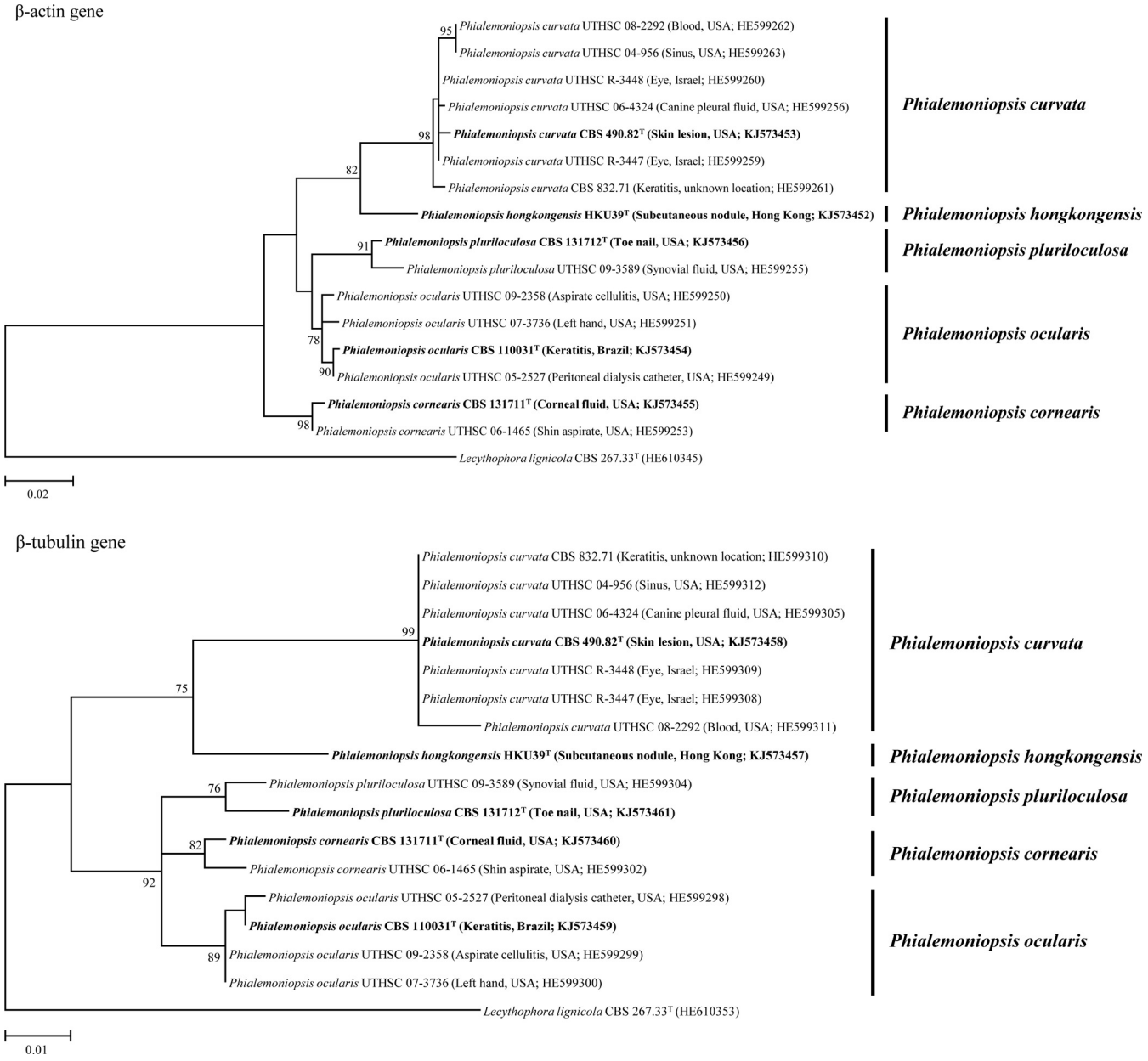

FIG 2 continued

preceding 6 months prior to admission. The patient had liver cirrhosis secondary to chronic hepatitis B for which he was receiving 0.5 mg of oral entecavir daily, newly diagnosed HLA-B27-positive ankylosing spondylitis, and active sputum smear-positive multilobar pulmonary tuberculosis for which he received 300 mg of oral isoniazid, 600 mg of rifampin, 1 g of ethambutol, and 500 mg of levofloxacin daily. An examination revealed a 4-cm by 3-cm by 3.5-cm, firm, nontender, and subcutaneous nodule with overlying inflammatory skin changes at the extensor surface of the right forearm. There was no discharge, bleeding, or ulceration. Chest radiography showed multilobar consolidations as a result of his active tuberculosis. Laboratory tests showed leukocytosis (13.8×10^9/liter; reference range, 4.4×10^9 to 10.1×10^9/liter) with neutrophilia (12.0×10^9/liter; reference range, 1.2×10^9 to 3.4×10^9/liter) and lymphopenia (0.7×10^9/liter; reference range, 1.2×10^9 to 3.4×10^9/liter), hyponatremia (127 mmol/liter; reference range, 136 to 148 mmol/liter), normal liver function tests and serum creatinine levels, and elevated C-reactive protein (10.2 mg/dl; reference range, <0.76 mg/dl) and erythrocyte sedimentation rate (107 mm/h; reference range, <20 mm/h).

The biopsy of the right forearm nodule showed multiple necrotizing granulomas with necrotic debris and acute inflammatory cells surrounded by epithelioid histiocytes and occasional multinucleated giant cells (Fig. 1a). Numerous fungal elements were identified in the necrotizing granulomas in the Grocott's methenamine silver-stained section (Fig. 1b and c). Gram and Ziehl-Neelsen stains did not show any bacteria or acid-fast bacilli. A culture of the biopsied tissue revealed tiny

TABLE 1 Growth rates of HKU39^T and its closely related species at different temperatures on PDA

Incubation temp (°C)	Growth rate (mean radii of fungal colonies [mm] after 21 days of incubation) of:				
	P. hongkongensis HKU39^T	*P. curvata* CBS 490.82^T	*P. ocularis* CBS 110031^T	*P. cornearis* CBS 131711^T	*P. pluriloculosa* CBS 131712^T
20	16.6	21.3	27.4	30.4	19.8
25	31.0	26.9	36.3	40.0	27.2
30	35.7	34.5	27.8	>45	35.3
35	6.0	10.0	0[a]	22.3	2.8
37	0[a]	2.6	0[a]	0[a]	0[b]

[a] No growth was observed in this test, but growth was observed on streaked agar plates.
[b] No growth was observed in this test, but weak growth was observed on streaked agar plates.

moldy colonies at the primary inoculation sites after 3 days of incubation at 37°C on horse blood agar, chocolate agar, MacConkey agar, and Sabouraud dextrose agar. The size of the colonies increased to about 7 mm in diameter after 1 week of incubation. No mycobacteria or contaminants were isolated. The patient was treated with 200 mg oral itraconazole twice daily. Unfortunately, his clinical condition deteriorated with progressive multiorgan failure and cord compression secondary to a collapsed T12 vertebral body, which was smear and culture positive for *Mycobacterium tuberculosis*, despite having received antituberculosis medications. An immunological work-up for underlying immunodeficiency syndromes associated with severe disseminated tuberculosis and opportunistic fungal infections, including a combined HIV antigen/antibody test and anti-interferon-gamma autoantibody test, were negative. He finally succumbed as a result of disseminated tuberculosis with multiorgan failure 1 month after admission.

ITS, partial 28S nrDNA, and partial β-actin and β-tubulin gene sequencing, comparative sequence identity analyses, and phylogenetic analyses. PCR of the ITS, partial 28S nrRNA, and partial β-actin and β-tubulin genes of HKU39^T and the reference strains showed bands at about 500 bp, 550 bp, 650 bp and 500 to 550 bp, respectively. Pairwise alignment showed the partial ITS of HKU39^T possessed 97.5% sequence identity to that of *P. pluriloculosa* CBS 131712^T, 97.3% sequence identity to that of *P. curvata* CBS 490.82^T, and 94.4 to 95.0% sequence identities to the ITS of other *Phialemoniopsis* species; the partial 28S nrDNA of HKU39^T possessed 99.5% sequence identity to that of *P. curvata* CBS 490.82^T and 97.3 to 98.2% sequence identities to the partial 28S nrDNA of other *Phialemoniopsis* species; the partial β-actin gene of HKU39^T possessed 93.6% sequence identity to that of *P. curvata* CBS 490.82^T and 91.0 to 91.8% sequence identities to the partial β-actin gene of other *Phialemoniopsis* species; and the partial β-tubulin gene of HKU39^T possessed 91.8% sequence identity to that of *P. curvata* CBS 490.82^T and 82.3 to 82.7% sequence identities to the partial β-tubulin gene of other *Phialemoniopsis* species. Phylogenetic analyses included 437 nucleotide positions of ITS, 432 nucleotide positions of partial 28S nrDNA, 646 nucleotide positions of the partial β-actin gene, and 373 nucleotide positions of partial β-tubulin gene and showed that HKU39^T occupies a unique phylogenetic position in the ITS, β-actin gene, and β-tubulin gene trees (Fig. 2). HKU39^T is most closely related to but distinct from *P. curvata*, suggesting it is a novel *Phialemoniopsis* species (Fig. 2).

Phenotypic characterization of HKU39^T. The API-ZYM test for HKU39^T showed that it was positive for *N*-acetyl-β-glucosaminidase, acid phosphatase, alkaline phosphatase, esterase (C4), esterase lipase (C8), β-glucosidase, leucine arylamidase, and naphthol-AS-BI-phosphohydrolase. The API 20 C AUX test for HKU39^T showed that it assimilated *N*-acetylglucosamine, L-arabinose, D-cellobiose, D-galactose, D-glucose, D-lactose, D-maltose, sucrose, D-trehalose, xylitol, and D-xylose. On PDA, HKU39^T grew at 20°C, 25°C, 30°C, and 35°C, with optimal growth occurring at 30°C (Table 1). No growth at 37°C was observed for the inoculated conidia, but growth at 37°C was observed for streaked plates.

MALDI-TOF MS. The protein mass spectra of HKU39^T and the other *Phialemoniopsis* species are shown in Fig. 3a. *P. curvata* CBS 490.82^T was identified as *Phialemonium* species (top match score, 2.184), whereas HKU39^T, *P. cornearis* CBS 131711^T, *P. ocularis* CBS 110031^T, and *P. pluriloculosa* CBS 131712^T were not identified by MALDI-TOF MS, which was probably due to the lack of their protein mass spectra in the MALDI Biotyper Reference Library 3.1.2.0 (Bruker Daltonics) MS database. Hierarchical cluster analysis showed that the protein mass spectrum of HKU39^T is most closely related to that of *P. pluriloculosa* CBS 131712^T (Fig. 3b).

Antifungal susceptibility of HKU39^T. The susceptibilities of HKU39^T to voriconazole, itraconazole, posaconazole, amphotericin B, fluconazole and flucytosine were 0.12 μg/ml, 0.5 μg/ml, 0.5 μg/ml, 1 μg/ml, 16 μg/ml, and >64 μg/ml, respectively. The azole drugs voriconazole, itraconazole, and posaconazole, as well as amphotericin B, showed high activity against HKU39^T, but the drugs fluconazole and flucytosine showed low activity against HKU39^T.

TAXONOMY

***Phialemoniopsis hongkongensis* Tsang, Chan, Ip, Ngan, Chen, Lau, Woo, sp. nov.** MycoBank accession no. MB 808614. Known distribution: Hong Kong. Etymology: named after Hong Kong, where the holotype was isolated. Specimen examined: Hong Kong; from the right forearm nodule biopsy of a human in 2007. Holotype: dried culture in the Herbarium of Biological Resource Center, National Institute of Technology and Evaluation (NBRC), Japan, with the accession no. NBRC H-13231. Ex-type cultures: HKU39^T (= NBRC 110143^T = NCPF 7868^T).

The colony on SDA was white to cream and smooth to velvety, with a diameter of about 35 mm with radial grooves after 3 weeks of incubation at 25°C (Fig. 4a). The reverse of colony was also white to cream, without diffusing pigment (Fig. 4b). Old cultures were dark brown (Fig. 4c). Microscopically, short adelophialides without basal septa were abundant with barely visible parallel col-

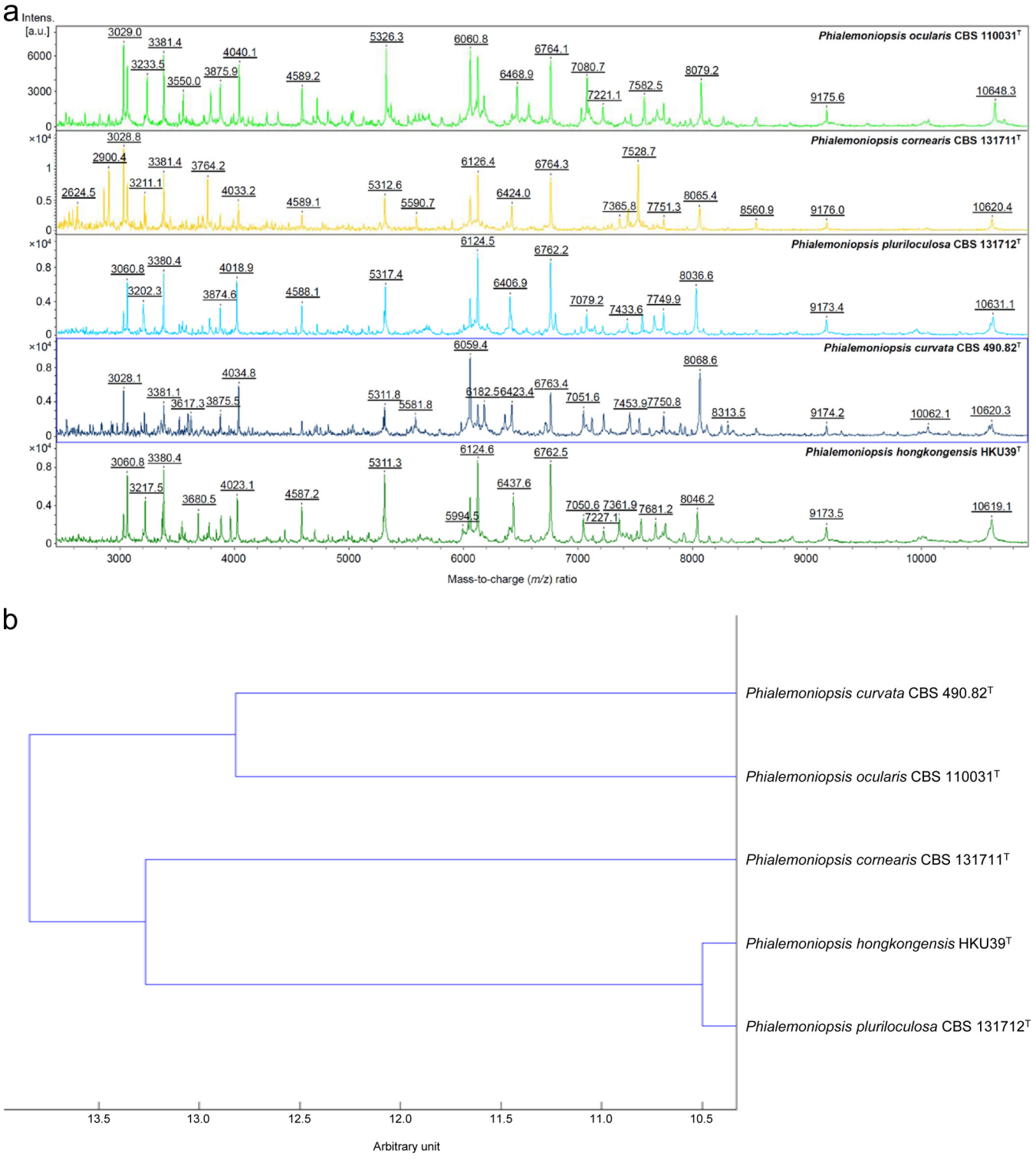

FIG 3 (a) MALDI-TOF mass spectra of *Phialemoniopsis* species. The numbers above the peaks indicate the *m/z* ratios of the respective cellular proteins. Intens., intensity; a.u. absorbance units. (b) Dendrogram generated from hierarchical cluster analysis of MALDI-TOF mass spectra of *Phialemoniopsis* species.

larettes. Discrete phialides with basal septa were less common and they were long, cylindrical, and tapered slightly toward the apex (Fig. 4d). Polyphialides were occasionally observed (Fig. 4e). Conidia were produced by phialides, positioned intercalary, and formed along hyaline, smooth-walled hyphae with a width of around 1 to 1.5 μm (Fig. 4f and h). The conidia were small, hyaline, cylindrical, oval or rod-shaped, slightly curved, and smooth-walled in slimy heads, with a size of about 2 to 3 by 1 to 2 μm

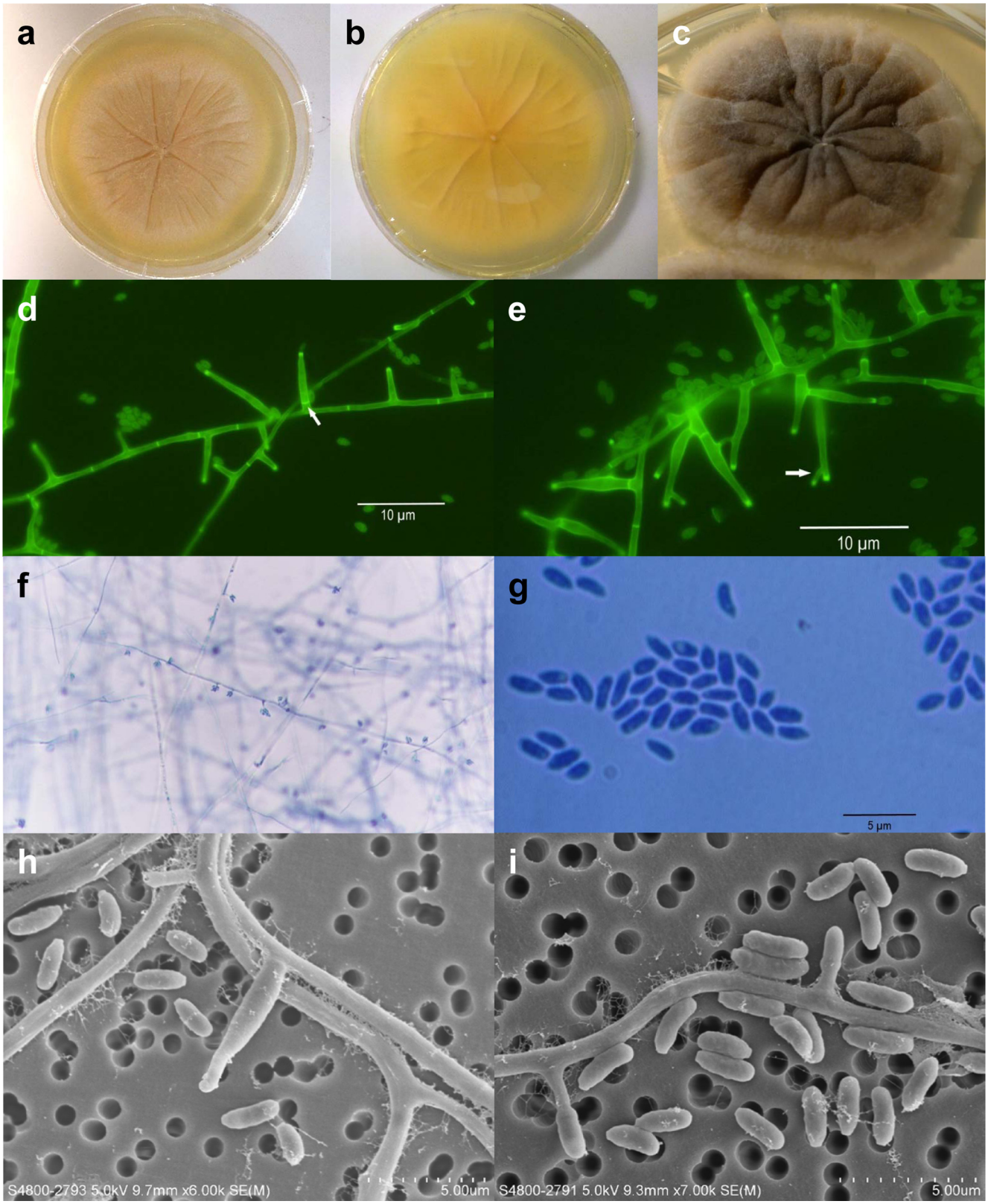

FIG 4 Colony surface (a) and reverse of colony (b) on SDA after 3 weeks of incubation at 25°C. (c) Colony surface on SDA after 5 weeks of incubation at 25°C. (d) Discrete phialide with basal septum (arrow) (light micrograph, calcofluor white stain). (e) Polyphialide (arrow) (light micrograph, calcofluor white stain). (f) Intercalary conidia along hyaline hyphae (light micrograph, lactophenol cotton blue stain). (g) Detail of conidia (light micrograph, lactophenol cotton blue stain). (h) Conidia and intercalary adelophialides along the hyphae (scanning electron micrograph). (i) Monophialide with inconspicuous collarette along the smooth-walled hyphae and a newly formed conidium produced through the opening of phialide (scanning electron micrograph).

(Fig. 4g and i). No chlamydospores were observed after 4 weeks of incubation on low-nutrient medium.

Although *P. hongkongensis* is morphologically similar to *P. curvata*, it can be distinguished from *P. curvata* by its shorter conidia. *P. hongkongensis* can also be distinguished from other *Phialemoniopsis* species by the absence of chlamydospores. Genotypically, *P. hongkongensis* can be well distinguished from other *Phialemoniopsis* species by sequencing the ITS, β-actin gene, and β-tubulin gene.

DISCUSSION

We report here the isolation of HKU39^T in pure growth from a patient biopsy specimen of a right forearm nodule. The clinical significance of the fungus was evident by the demonstration of fungal invasion to the patient's tissue as well as granulomatous inflammatory reactions in the histological sections of the biopsied specimen. A culture of the biopsy specimen also showed colonies at the primary inoculum on all agar plates inoculated with the specimen, supporting that the isolate was from the clinical specimen instead of due to contamination. The sequencing of four different DNA regions commonly used for phylogenetic studies, including the ITS, 28S nrDNA, β-actin gene, and β-tubulin gene, and phylogenetic analyses showed that HKU39^T stood out as a unique branch that was distinct from the other *Phialemoniopsis* species in the ITS, β-actin gene, and β-tubulin gene trees generated (Fig. 2). Although HKU39^T was most closely related to *P. curvata* in the phylogenetic trees, the clustering of HKU39^T to *P. curvata* was supported by bootstrap values of <90 (Fig. 2). Moreover, comparative sequence identity analyses showed that the partial ITS sequence of HKU39^T was the most similar to that of *P. pluriloculosa*, but the partial sequences of the other three gene loci of HKU39^T were the most similar to those of *P. curvata*. Notably, a hierarchical cluster analysis of the MALDI-TOF mass spectra revealed that HKU39^T was most closely related to *P. pluriloculosa* instead of *P. curvata* (Fig. 3). All these results supported that HKU39^T should belong to a novel *Phialemoniopsis* species distinct from any other members of this genus, and we propose a novel species, *P. hongkongensis*, to accommodate HKU39^T. Since *Phialemoniopsis* species are ubiquitous and the patient was a construction site worker who was prone to unnoticed repeated minor traumas, we speculate that he had probably acquired the infection via direct inoculation of the fungus to his forearm through one of the trauma events. As for antifungal susceptibility, the susceptibility profile of HKU39^T is similar to those of *P. curvata* and *P. ocularis* (15, 23). The azole drugs voriconazole, itraconazole, and posaconazole, as well as amphotericin B, showed high activity against all these three *Phialemoniopsis* species, but the drugs fluconazole and flucytosine showed low activity against these species. Therefore, itraconazole, voriconazole, posaconazole, and/or amphotericin B can be considered the drugs of choice for the treatment of *Phialemoniopsis* infections.

The fact that *P. curvata* exhibits much better growth at 37°C is important for its association with more cases of systemic mycoses, whereas *P. hongkongensis* and other *Phialemoniopsis* species are causes of relatively superficial infections. When the taxonomy of the genus *Phialemonium* was reviewed in 2013 using molecular phylogenetics, *Phialemonium curvatum* and *Sarcopodium oculorum* were transferred to a new genus, *Phialemoniopsis*, and obtained their current names, *P. curvata* and *P. ocularis*, respectively; two other new species (*P. cornearis* and *P. pluriloculosa*) were also established under this genus (1). Among these four *Phialemoniopsis* species, only *P. curvata* grew at 37°C, whereas the other three *Phialemoniopsis* species, only their streaked plate cultures, but not conidia, grew well at 37°C (Table 1). Notably, previous reports have shown that *P. curvata* is a much more common cause of deep-seated systemic mycoses (7, 9, 10, 12, 17, 20–24) than are the other *Phialemoniopsis* species. As for the other *Phialemoniopsis* species, they were usually recovered from more superficial body sites (1, 15, 25), where the temperature is usually lower than the core body temperature (<37°C). We speculate that this is because the conidia of these three *Phialemoniopsis* species do not germinate beyond 35°C (30°C for *P. ocularis*), making them uncommon causes of systemic mycosis. Interestingly, in the present study, we also showed that only the streaked plate cultures, but not the conidia of *P. hongkongensis*, grew well at 37°C, and *P. hongkongensis* was also associated with a relatively superficial necrotizing granulomatous infection of the forearm.

Multilocus sequencing is so far the most reliable way to distinguish between *Phialemoniopsis* and other morphologically similar fungal genera, as well as to identify various members of *Phialemoniopsis* down to the species level. It has been suggested that infections by *Phialemoniopsis* species might be underreported due to the misidentification of clinical *Phialemoniopsis* isolates, which are morphologically similar to fungi belonging to other genera more commonly found in human infections, such as *Acremonium* and *Fusarium* (13). As for identification to the species level, the morphological differences among the various *Phialemoniopsis* species are even more subtle and unreliable. As revealed by the ITS tree generated in this study (Fig. 2), a number of *Phialemoniopsis* strains, which were identified as *Phialemonium* cf. *curvatum* or *Phialemonium* sp. by other authors (P. K. Balne, S. Sharma, A. K. Reddy, P. Garg, and C. Kannabiran, unpublished data), should actually be *P. cornearis* (strains LVPEI.H1787_11, LVPEI.H3921_11, LVPEI.H4100_11, and LVPEI.H4305_11) or *P. pluriloculosa* (strain LVPEI.B52_12). Moreover, as revealed in the 28S nrDNA tree generated in this study (Fig. 2), the strain CBS 365.61, which was identified as *P. curvatum*, may represent another novel *Phialemoniopsis* species. As for the potential use of MALDI-TOF MS for fungal identification, *P. curvata* was correctly identified as a species in the genus *Phialemonium*, to which it previously belonged. Therefore, theoretically, the other *Phialemoniopsis* species might also be correctly identified, provided that enough protein mass spectra of each *Phialemoniopsis* species are included in the MALDI-TOF MS database and the database is up-to-date (37, 39).

ACKNOWLEDGMENTS

This work is partly supported by the Health and Medical Research Fund, Food and Health Bureau, the Government of the Hong Kong SAR, Hong Kong, and the Small Project Funding Scheme and Strategic Research Theme Fund, The University of Hong Kong, Hong Kong.

We thank the curators of CBS-KNAW Fungal Biodiversity Centre, the Netherlands, for providing the reference strains. We also thank Sayaka Ban, fungal curator of the NBRC, Japan, for helping preserve the holotype herbarium specimen and the ex-type culture and Adrien Szekely, curator of National Collection of Pathogenic Fungi (NCPF), Public Health England (PHE) Mycology Reference Laboratory, United Kingdom, for helping preserve the ex-type culture.

We declare no conflicts of interest.

REFERENCES

1. **Perdomo H, García D, Gené Cano JJ, Sutton DA, Summerbell R, Guarro J.** 2013. *Phialemoniopsis*, a new genus of *Sordariomycetes*, and new species of *Phialemonium* and *Lecythophora*. Mycologia **105:**398–421. http://dx.doi.org/10.3852/12-137.
2. **Gams W, McGinnis MR.** 1983. *Phialemonium*, a new anamorph genus intermediate between *Phialophora* and *Acremonium*. Mycologia **75:**977–987. http://dx.doi.org/10.2307/3792653.
3. **Crane PE, Chakravarty P, Hutchison LJ, Hiratsuka Y.** 1996. Wood-degrading capabilities of microfungi isolated from *Populus tremuloides*. Mater. Organismen. **30:**33–44.
4. **Halleen F, Mostert L, Crous PW.** 2007. Pathogenicity testing of lesser-known vascular fungi of grapevines. Australas. Plant Pathol. **36:**277–285. http://dx.doi.org/10.1071/AP07019.
5. **Suada IK, Suhartini DMWY, Sunariasih NPL, Wirawan IGP, Chun KW, Cha JY, Ohga S.** 2012. Ability of endophytic fungi isolated from rice to inhibit *Pyricularia oryzae*-induced rice blast in Indonesia. J. Fac. Agr. Kyushu Univ. **57:**51–53.
6. **King D, Pasarell L, Dixon DM, McGinnis MR, Merz WG.** 1993. A phaeohyphomycotic cyst and peritonitis caused by *Phialemonium* species and a reevaluation of its taxonomy. J. Clin. Microbiol. **31:**1804–1810.
7. **Guarro J, Nucci M, Akiti T, Gené Cano J, Barreiro MDGC, Aguilar C.** 1999. *Phialemonium* fungemia: two documented nosocomial cases. J. Clin. Microbiol. **37:**2493–2497.
8. **Heins-Vaccari EM, Machado CM, Saboya RS, Silva RL, Dulley FL, Lacaz CS, Freitas Leite RS, Hernandez Arriagada GL.** 2001. *Phialemonium curvatum* infection after bone marrow transplantation. Rev. Inst. Med. Trop. Sao Paulo **43:**163–166. http://dx.doi.org/10.1590/S0036-46652001000300009.
9. **Proia LA, Hayden MK, Kammeyer PL, Ortiz J, Sutton DA, Clark T, Schroers HJ, Summerbell RC.** 2004. *Phialemonium*: an emerging mold pathogen that caused 4 cases of hemodialysis-associated endovascular infection. Clin. Infect. Dis. **39:**373–379. http://dx.doi.org/10.1086/422320.
10. **Dan M, Yossepowitch O, Hendel D, Shwartz O, Sutton DA.** 2006. *Phialemonium curvatum* arthritis of the knee following intra-articular injection of a corticosteroid. Med. Mycol. **44:**571–574. http://dx.doi.org/10.1080/13693780600631883.
11. **Sutton DA, Wickes BL, Thompson EH, Rinaldi MG, Roland RM, Libal MC, Russell K, Gordon S.** 2008. Pulmonary *Phialemonium curvatum* phaeohyphomycosis in a standard poodle dog. Med. Mycol. **46:**355–359. http://dx.doi.org/10.1080/13693780701861470.
12. **Rao CY, Pachucki C, Cali S, Santhiraj M, Krankoski KL, Noble-Wang JA, Leehey D, Popli S, Brandt ME, Lindsley MD, Fridkin SK, Arduino MJ.** 2009. Contaminated product water as the source of *Phialemonium curvatum* bloodstream infection among patients undergoing hemodialysis. Infect. Control Hosp. Epidemiol. **30:**840–847. http://dx.doi.org/10.1086/605324.
13. **Perdomo H, Sutton DA, García D, Fothergill AW, Gené J, Cano J, Summerbell RC, Rinaldi MG, Guarro J.** 2011. Molecular and phenotypic characterization of *Phialemonium* and *Lecythophora* isolates from clinical samples. J. Clin. Microbiol. **49:**1209–1216. http://dx.doi.org/10.1128/JCM.01979-10.
14. **Higginbotham S, Wong WR, Linington RG, Spadafora C, Iturrado L, Arnold AE.** 2014. Sloth hair as a novel source of fungi with potent anti-parasitic, anti-cancer and anti-bacterial bioactivity. PLoS One **9:**e84549. http://dx.doi.org/10.1371/journal.pone.0084549.
15. **Guarro J, Höfling-Lima AL, Gené J, De Freitas D, Godoy P, Zorat-Yu ML, Zaror L, Fischman O.** 2002. Corneal ulcer caused by the new fungal species *Sarcopodium oculorum*. J. Clin. Microbiol. **40:**3071–3075. http://dx.doi.org/10.1128/JCM.40.8.3071-3075.2002.
16. **Freda R, Dal Pizzol MM, Fortes Filho JB.** 2011. *Phialemonium curvatum* infection after phacoemulsification: a case report. Eur. J. Ophthalmol. **21:**834–836. http://dx.doi.org/10.5301/EJO.2011.8360.
17. **Strahilevitz J, Rahav G, Schroers HJ, Summerbell RC, Amitai Z, Goldschmied-Reouven A, Rubinstein E, Schwammenthal Y, Feinberg MS, Siegman-Igra Y, Bash E, Polacheck I, Zelazny A, Howard SJ, Cibotaro P, Shovman O, Keller N.** 2005. An outbreak of *Phialemonium* infective endocarditis linked to intracavernous penile injections for the treatment of impotence. Clin. Infect. Dis. **40:**781–786. http://dx.doi.org/10.1086/428045.
18. **Zayit-Soudry S, Neudorfer M, Barak A, Loewenstein A, Bash E, Siegman-Igra Y.** 2005. Endogenous *Phialemonium curvatum* endophthalmitis. Am. J. Ophthalmol. **140:**755–757. http://dx.doi.org/10.1016/j.ajo.2005.04.037.
19. **Weinberger M, Mahrshak I, Keller N, Goldscmied-Reuven A, Amariglio N, Kramer M, Tobar A, Samra Z, Pitlik SD, Rinaldi MG, Thompson E, Sutton D.** 2006. Isolated endogenous endophthalmitis due to a sporodochial-forming *Phialemonium curvatum* acquired through intracavernous autoinjections. Med. Mycol. **44:**253–259. http://dx.doi.org/10.1080/13693780500411097.
20. **Osherov A, Schwammenthal E, Kuperstein R, Strahilevitz J, Feinberg MS.** 2006. *Phialemonium curvatum* prosthetic valve endocarditis with an unusual echocardiographic presentation. Echocardiography. **23:**503–505. http://dx.doi.org/10.1111/j.1540-8175.2006.00249.x.
21. **Zou Y, Bi Y, Bu H, He Y, Guo L, Shi D.** 2014. Infective meningitis caused by *Phialemonium curvatum*: a case report. J. Clin. Microbiol. http://dx.doi.org/10.1128/JCM.00419-14.
22. **Schønheyder HC, Jensen HE, Gams W, Nyvad O, Van Nga P, Aalbaek B, Stenderup J.** 1996. Late bioprosthetic valve endocarditis caused by *Phialemonium* aff. *curvatum* and *Streptococcus sanguis*: a case report. J. Med. Vet. Mycol. **34:**209–214. http://dx.doi.org/10.1080/02681219680000351.
23. **Rivero M, Hidalgo A, Alastruey-Izquierdo A, Cía M, Torroba L, Rodríguez-Tudela JL.** 2009. Infections due to *Phialemonium* species: case report and review. Med. Mycol. **47:**766–774. http://dx.doi.org/10.3109/13693780902822800.
24. **Persy B, Vrelust I, Gadisseur A, Ieven M.** 2011. *Phialemonium curvatum* fungaemia in an immunocompromised patient: case report. Acta Clin. Belg. **66:**384–386.
25. **Desoubeaux G, García D, Bailly E, Augereau O, Bacle G, De Muret A, Bernard L, Cano-Lira JF, Garcia-Hermoso D, Chandenier J.** 2014. Subcutaneous phaeohyphomycosis due to *Phialemoniopsis ocularis* successfully treated by voriconazole. Med. Mycol. Case Rep. **5:**4–8. http://dx.doi.org/10.1016/j.mmcr.2014.04.001.
26. **Woo PCY, Ngan AH, Chui HK, Lau SK, Yuen KY.** 2010. Agar block smear preparation: a novel method of slide preparation for preservation of native fungal structures for microscopic examination and long-term storage. J. Clin. Microbiol. **48:**3053–3061. http://dx.doi.org/10.1128/JCM.00917-10.
27. **Woo PC, Tam EW, Chong KT, Cai JJ, Tung ET, Ngan AH, Lau SK, Yuen KY.** 2010. High diversity of polyketide synthase genes and the melanin biosynthesis gene cluster in *Penicillium marneffei*. FEBS J. **277:**3750–3758. http://dx.doi.org/10.1111/j.1742-4658.2010.07776.x.
28. **Woo PC, Ngan AH, Tsang CC, Ling IW, Chan JF, Leung SY, Yuen KY, Lau SK.** 2013. Clinical spectrum of *Exophiala* infections and a novel *Exophiala* species, *Exophiala hongkongensis*. J. Clin. Microbiol. **51:**260–267. http://dx.doi.org/10.1128/JCM.02336-12.
29. **White T, Bruns T, Lee S, Taylor J.** 1990. Amplification and direct sequencing of fungal ribosomal RNA genes for phylogenetics, p 315–322. *In* Innis M, Gelfand D, Shinsky J, White T (ed), PCR protocols: a guide to methods and applications. Academic Press, San Diego, CA.
30. **O'Donnell K.** 1993. *Fusarium* and its near relatives, p 225–233. *In* Reynolds DR, Taylor JW (ed), The fungal holomorph: mitotic, meiotic and pleomorphic speciation in fungal systematics. CAB International, Wallingford, United Kingdom.
31. **Cruse M, Telerant R, Gallagher T, Lee T, Taylor JW.** 2002. Cryptic species in *Stachybotrys chartarum*. Mycologia **94:**814–822. http://dx.doi.org/10.2307/3761696.
32. **Hall TA.** 1999. BioEdit: a user-friendly biological sequence alignment editor and analysis program for Windows 95/98/NT. Nucleic Acids Symp. Ser. (Oxf.) **41:**95–98.
33. **Edgar RC.** 2004. MUSCLE: multiple sequence alignment with high accuracy and high throughput. Nucleic Acids Res. **32:**1792–1797. http://dx.doi.org/10.1093/nar/gkh340.
34. **Castresana J.** 2000. Selection of conserved blocks from multiple alignments for their use in phylogenetic analysis. Mol. Biol. Evol. **17:**540–552. http://dx.doi.org/10.1093/oxfordjournals.molbev.a026334.
35. **Talavera G, Castresana J.** 2007. Improvement of phylogenies after removing divergent and ambiguously aligned blocks from protein sequence alignments. Syst. Biol. **56:**564–577. http://dx.doi.org/10.1080/10635150701472164.
36. **Tamura K, Stecher G, Peterson D, Filipski A, Kumar S.** 2013. MEGA6: Molecular Evolutionary Genetics Analysis version 6.0. Mol. Biol. Evol. **30:**2725–2729. http://dx.doi.org/10.1093/molbev/mst197.
37. **Lau SK, Tang BS, Teng JL, Chan TM, Curreem SO, Fan RY, Ng RH, Chan JF, Yuen KY, Woo PC.** 2014. Matrix-assisted laser desorption ionisation time-of-flight mass spectrometry for identification of clinically significant

bacteria that are difficult to identify in clinical laboratories. J. Clin. Pathol. **67:**361–366. http://dx.doi.org/10.1136/jclinpath-2013-201818.

38. **Tsang CC, Chan JFW, Trendell-Smith NJ, Ngan AH, Ling IW, Lau SK, Woo PC.** 2014. Subcutaneous phaeohyphomycosis in a patient with IgG4-related sclerosing disease caused by a novel ascomycete, *Hongkongmyces pedis* gen. et sp. nov.: first report of human infection associated with the family *Lindgomycetaceae*. Med. Mycol., in press.

39. **Tam EW, Chen JH, Lau EC, Ngan AH, Fung KS, Lee KC, Lam CW, Yuen KY, Lau SK, Woo PC.** 2014. Misidentification of *Aspergillus nomius* and *Aspergillus tamarii* as *Aspergillus flavus*: characterization by internal transcribed spacer, β-tubulin, and calmodulin gene sequencing, metabolic fingerprinting, and matrix-assisted laser desorption ionization–time of flight mass spectrometry. J. Clin. Microbiol. **52:**1153–1160. http://dx.doi.org/10.1128/JCM.03258-13.